10.5005/jp-journals-10018-1050
CASE REPORT

A Case of *de novo* Hepatitis B Complicated due to Lack of Comprehensive Interventional Approach

Hiroshi Onji, Youhei Koizumi, Masakazu Hanayama, Sheikh Mohammad Fazle Akbar, Masashi Hirooka, Yoshio Tokumoto, Masanori Abe, Yoichi Hiasa, Mamoru Aoto, Noriaki Mitsuda, Morikazu Onji

ABSTRACT

Here, we report a case of *de novo type B hepatitis* in a patient with hepatitis B surface antigen (HBsAg) negative but positive for low titer of anti-HBc antibody (anti-HBc titer; dilution 200; negative). As the disease was anticipated in advance, the patient received nucleos(t)ide analogs, but *de novo type B hepatitis* was developed, because of discontinuation of antiviral drugs.

A 59-year-old male with a history of T cell rich diffuse large B-cell lymphoma (DLBCL) and was treated with rituximab plus cyclophosphomide, doxorubicin, vincristine and prednisolone (R-CHOP). The patient responded to anticancer therapy and his complete responder status was confirmed by PET-CT on October 4, 2010. As the patient was expressing low levels of anti-HBc (anti-HBc titer; dilution 200-negative), he was given lamivudine to block HBV reactivation, but the drug was continued after 1 year due to apparent improvement. Stoppage of antiviral drug resulted in detectable HBV DNA and evidences of liver damages and he was referred to our department for specialized consultation about liver-related complications. He was given entecavir at a dose of 1 gm/day from May 2012. However, the parameters of liver function test showed anomaly indicating progressive liver damages. Subsequently, he was given steroid pulse therapy with 1,000 mg of prednisolone and tapered successively. The levels of HBV DNA decreased and parameters of liver function test were improved. A biopsy specimen taken in July 2012 showed the findings compatible with resolved acute hepatitis. To prevent *de novo type B hepatitis*, critical observation and timely management of the patients are necessary. The administration with nucleoside analogs at least 1 year after R-CHOP therapy is recommended in guideline of Japanese Society of Hepatology. However, we should reconsider the term of administration with nucleoside analogs after R-CHOP therapy.

Keywords: HBV, *de novo* hepatitis, Rituximab, HBV reactivation, Nucleoside analogs, Interdisciplinary approach.

How to cite this article: Onji H, Koizumi Y, Hanayama M, Akbar SMF, Hirooka M, Tokumoto Y, Abe M, Hiasa Y, Aoto M, Mitsuda N, Onji M. A Case of *de novo* Hepatitis B Complicated due to Lack of Comprehensive Interventional Approach. Euroasian J Hepato-Gastroenterol 2012;2(2):122-125.

Source of support: Nil

Conflict of interest: None

INTRODUCTION

It is estimated that 2 billion people worldwide have been infected with Hepatitis B Virus (HBV).[1] In Japan, it is reported that 23.2% of blood donors are positive for HBc antibody and/or HBs antibody.[2] Reactivation of HBV is a well-recognized complication in hepatitis B surface antigen (HBsAg) positive patients who are undergoing immunosuppressive chemotherapy including anti-CD20 antibody for malignancies. The clinical manifestation ranges from subclinical hepatitis to severe and potentially fatal fulminant hepatic failure.[3-6] In this decade, HBV reactivation has been observed in patients with resolved infection who have undergone intensive immunosuppressive chemotherapy, such as rituximab plus steroid-containing chemotherapy. This usually happens in patients expressing HBsAg and HBV DNA in peripheral blood. Here, we report a case of *de novo* type B hepatitis in a patient with HBsAg negative but positive for low titer of anti-HBc antibody (anti-HBc titer; dilution 200; negative). The patient developed *de novo* type B hepatitis even after the prophylactic administration of nucleos(t)ide analogs for more than 1 year and 4 months after stopping of R-CHOP therapy. The present case report would contribute about importance of comprehensive approach to prevent *de novo* hepatitis. Also, some insights would be provided about duration of antiviral therapy in these circumstances.

CASE REPORT

A 59-year-old male with a history of T cell rich diffuse large B-cell lymphoma (DLBCL) is presented. The patient revealed a history of general malaise, low-grade fever, skin itching and weight loss from February 2010. Lymph node enlargement was shown in the right cervix, and biopsy specimen of right cervical region showed T-cell rich DLBCL (stage III). The patient was administered an anticancer therapy with rituximab plus cyclophosphomide, doxorubicin, vincristine and prednisolone (R-CHOP) for eight courses from March 2010 to August 2010. The patient responded to anticancer therapy and his complete responder status was confirmed by PET-CT on October 4, 2010. As the patient was expressing low levels of anti-HBc (anti-HBc titer; dilution 200 negative), he was given lamivudine to block HBV reactivation from May 2010. Administration of lamivudine was stopped in October 26, 2011 after the prophylactic administration of lamivudine for more than 1 year and 4 months after stopping of R-CHOP therapy. Subsequently, HBV DNA became detectable in the sera from February 29, 2012. The amount of HBV DNA was increased to 8.4 log copies/ml on May 30, 2012. Just after

consulting with hepatologist, he was administered entecavir at a dose of 1 gm/day. However, the parameters of liver function test showed downhill terns and referred to us. Physical findings on admission: Height: 174 cm; weight: 58.3 kg, BMI: 19.3 he was not icteric; lung; no abnormality detected. The abdomen was flat, smooth, soft and non-tender. The liver and spleen was not palpable. There was no flapping tremor. Laboratory data was shown in Table 1. The patient showed general malaise and loss of appetite. Hepatomegaly and yellowing of the eyes were not shown. The parameters of liver function test in June 25, 2012, was AST, 322 U/l; ALT, 390 U/l; LDH, 373 U/l; ALP, 283 U/l, γ-GTP, 38 U/l, total bilirubin; 0.8 gm/dl; direct bilirubin, 0.1 mg/dl and prothrombin time, 76.8 %. The level of HBV DNA was 6.1 log copies/ml (HBV genotype B). The patient was expressing HBsAg (36,360 IU/ml) and HBeAg in the sera. HBsAg became for positive on June 30, 2012. His HBV was wild-type. Positivity of HBV-DNA was observed after 1 year and 7 months, HBs antigen became positive after 1 year and 10 months, abnormality of AST/ALT was after 1 year and 11 months after cease of R-CHOP therapy. Clinical course of present case was shown in Figure 1. In spite of antiviral therapy, progressive liver damages continued as evident from values of ALT and AST. In June 2012, steroid pulse therapy was started with 1,000 mg of prednisolone and tapered successively. The levels of HBV DNA, AST and ALT fell due to integrated therapy. The levels of HBV-DNA decreased and subjective symptoms disappeared, and the parameters of liver function test became normalized. A liver biopsy was done in July 30, 2012, the liver specimen showed in Figures 2A and B. Liver-cell damage, cell death and inflammatory cells infiltration were seen predominantly in central area, but there was no bridging necrosis. There was few abnormal finding in periportal area. These findings indicate resolved acute hepatitis. The patient discharged from hospital on 15th August 2012.

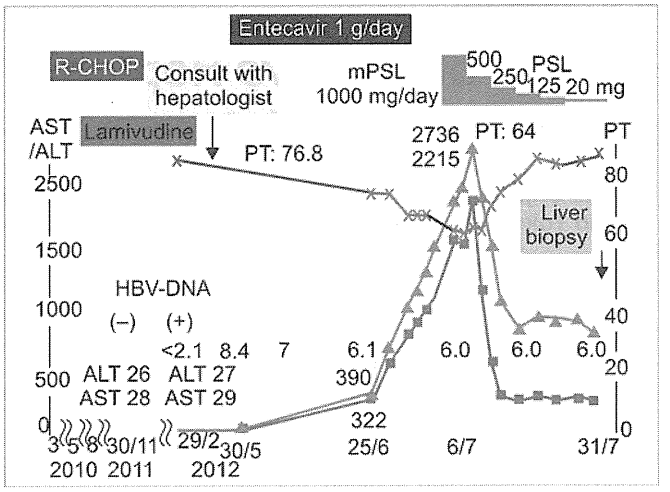

Fig. 1: Clinical course of present case

DISCUSSION

With the advent of immunosuppressive agents, the uses of these drugs have been related to some incidences of death because of reactivation of HBV and acute hepatic failure. Previous reports have clarified that this combination therapy can lead to acute hepatic failure and even death. For this reason, clinicians need to be aware of HBV reactivation not only in patients with current infection but also in those with resolved infection who are undergoing intensive immunosuppressive therapy.

The *de novo* hepatitis B could occur after the reactivation of HBV, when HBs antigen and HBV-DNA negative, but antipositive patients are treated with immunosuppressive agents. It becomes evident that the prophylactic administration of nucleos(t)ide analogs is very effective against the reactivation of HBV and occurrence of *de novo* hepatitis.[7-9] To prevent *de novo* type B hepatitis, critical observation and timely management of the patients are necessary. Also, multidisciplinary approach is necessary. A guideline of Japanese Society of Hepatology to manage *de novo* hepatitis and reactivation of HBV during and after

Table 1: Laboratory findings on administration day (June 25th, 2012)

WBC	4200/μl	AST	322 U/l	HBV-DNA	6.1 log copies/ml
RBC	3.82 × 10^6/μl	ALT	390 U/l	HBs Ag	(+)
HGB	12.9 g/dl	LDH	373 U/l	HBe Ag	(+) 245
HCT	37.7%	ALP	283 U/l	HBe Ab	(–)
PLT	15.3 × 10^4/μl	γ-GTP	38 U/l	HBc Ab	X1 (±) 53%
PT	76.8%	Na	142 mEq/l		X200 (–)
		K	3.6 mEq/l	HBV genotype	B
TP	6.3 g/dl	Cl	103 mEq/l	HBV YMDD	
Alb	4.0 g/dl	BUN	14 mg/dl	Lamivudine	Mutant (–)
TB	0.8 g/dl	Cre	0.78 mg/dl	HBV precore	Wild type
DB	0.1 g/dl	UA	6.7 mg/dl	Core promoter	Wild type
CHE	344 U/l	CRP	0.33 mg/dl		
		Glu	102 mg/dl		

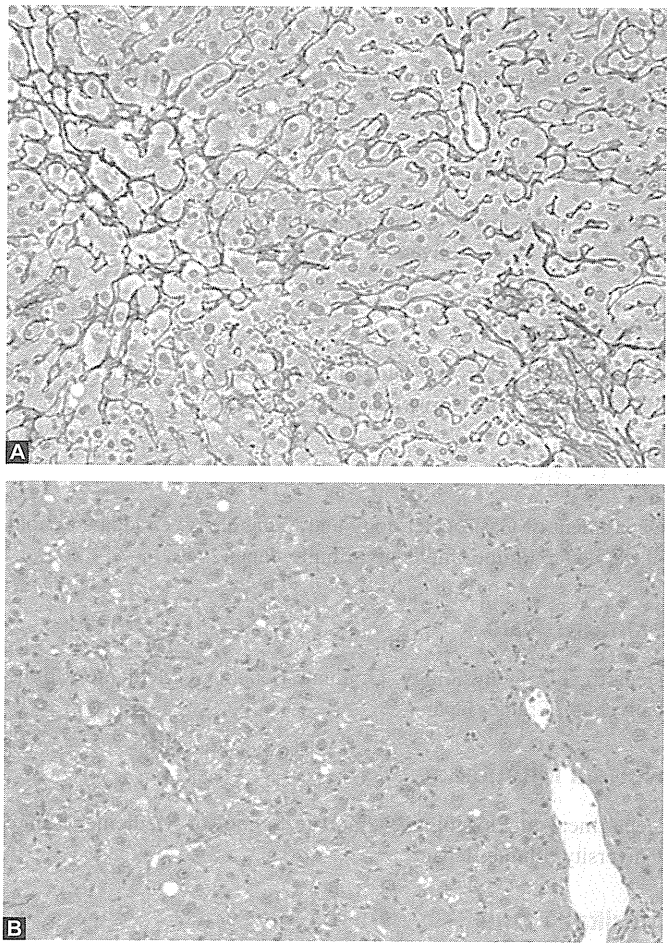

Figs 2A and B: Biopsy specimen on the 63rd clinical day. Liver-cell damage, cell death and inflammatory cells infiltration were seen predominantly in central area, but there was no bridging necrosis. These findings indicate resolved acute hepatitis

immunosuppressive drugs, was reported and became popular to use it in Japan.[10,11] Japanese guideline that prevents reactivation *de novo* hepatitis of HBV is widely used not only by hepatologist but also by hematologist and rheumatologist. Similar guidelines were reported from Europe and USA.[12-14] Japanese guideline described that prophylactic administration should be continued for at least 1 year. In present case, the patient was treated with lamivudine for 1 year and 4 months after the case of R-CHOP therapy. But after stopping administration of lamivudine, HBV-DNA became positive within 4 months, and HBsAg became positive in 7 months, then acute hepatitis occurred. It means that, in this case, the occurrence of acute hepatitis was not prevented with the administration of lamivudine for 1 year and 4 months after stopping R-CHOP therapy. Though the Japanese guideline described that nucleos(t)ide analogs should be administered 'at least 1 year', the present case showed that nucleoside analogs for more than 1 year. We think that this case is valuable to know when we should stop the prophylactic administration of nucleos(t)ide analogs and how we should observe the patient after the stop of administration. This has become an emerging problem in every field of clinical medicine.[15]

CONCLUSION

Prolonged use of antiviral drugs seems to be necessary in immune suppressed patients with previous history of HBV infection. Also, a comprehensive approach is needed to tackle these patients. Periodic updating of therapeutic recommendations is also a necessity.

ACKNOWLEDGMENT

This study was supported in part by a Grant-in-Aid from the Japanese Ministry of Health, Welfare, and Labor, about Research Group for the long-term prognosis of anti-HBe antibody positive asymptomatic HBV carriers in Japan.

REFERENCES

1. Lee WM. Hepatitis B virus infection. N Engel J Med 1997; 337:1733-45.
2. Kusumoto S, Tanaka Y, Mizokami M, Ueda R. Reactivation of hepatitis B virus following systemic chemotherapy for malignant lymphoma. Int J Hematol 2009;90:13-23.
3. Sera T, Hiasa Y, Michitaka K, Konishi I, et al. Anti-HBs-positive liver failure due to hepatitis B virus reactivation induced by rituximab. Inter Med 2006;45:721-24.
4. Nakamura Y, Motokura T, Fujita A, Yamashita T, Ogata E. Severe hepatitis related to chemotherapy in hepatitis B virus carriers with hematologic malignancies. Survey in Japan 1987-1991. Cancer 1996;78:2210-15.
5. Dervite I, Hober D, Morel P. Acute hepatitis B in a patient with antibodies to hepatitis B surface antigen who was receiving rituximab. N Engel J Med 2001;344:68-69.
6. Yeo W, Chan TC, Leung NW, et al. Hepatitis B virus reactivation in lymphoma patients with prior resolved hepatitis B undergoing anticancer therapy with or without rituximab. J Clin Oncol 2009; 27:605-11.
7. Yeo W, Chan PK, Ho WM, et al. Lamivudine for the prevention of hepatitis B virus reactivation in hepatitis B s-antigen seropositive cancer patients undergoing cytotoxic chemotherapy. J Clin Oncol 2004;22:927-34.
8. Hsu C, Hsiung CA, Su IJ, et al. A revisit of prophylactic lamivudine for chemotherapy-associated hepatitis B reactivation in non-Hodgkin's lymphoma: A randomized trial. Hepatology 2008;47:844-53.
9. Colonno RJ, Rose R, Baldick CJ, et al. Entecavir resistance is rare in nucleoside naïve patients with hepatitis B. Hepatology 2006;44:1656-65.
10. Tsubouchi H, Kumada H, Kiyosawa K, et al. Prevention of immunosuppressive therapy or chemotherapy-induced reactivation of hepatitis B virus infection. Joint report of the Intractable Liver Disease Study Group of Japan and the Japanese Study of the Standard Antiviral Therapy for Viral Hepatitis. Acta Hepatol Jpn 2009;50:38-42.
11. Oketani M, Ido A, Uto H, et al. Prevention of hepatitis B virus reactivation in patients receiving immunosuppressive therapy or chemotherapy. Heptol Res 2012;42:627-36.

12. European Association for the Study of the Liver. EASL clinical practice guidelines: Management of chronic hepatitis B. J Hepatol 2009;50:227-42.
13. Lok ASF, Ward JW, Perrillo RP, et al. Reactivation of hepatitis B during immunosuppressive therapy: Potentially fatal yet preventable. Ann Int Med 2012;156:743-45.
14. Lubel JS, Testro AG, Angus PW. Hepatitis B virus reactivation following immunosuppressive therapy: Guidelines for prevention and management. Internal Med J 2007;37:705-12.
15. Urata Y, Uesato R, Tanaka D, et al. Prevalence of reactivation of hepatitis B virus replication in rheumatoid arthritis patients. Mod Rheumatol 2011;21:16-23.

ABOUT THE AUTHORS

Hiroshi Onji

Department of Physiology, Graduate School of Medicine, Ehime University, Ehime, Japan

Youhei Koizumi

Department of Gastroenterology and Metabology, Graduate School of Medicine, Ehime University, Ehime, Japan

Masakazu Hanayama

Postgraduate Clinical Training Center, Graduate School of Medicine Ehime University, Ehime, Japan

Sheikh Mohammad Fazle Akbar

Department of Medical Sciences, Toshiba General Hospital, Tokyo Japan

Masashi Hirooka

Department of Gastroenterology and Metabology, Graduate School of Medicine, Ehime University, Ehime, Japan

Yoshio Tokumoto

Department of Gastroenterology and Metabology, Graduate School of Medicine, Ehime University, Ehime, Japan

Masanori Abe

Department of Gastroenterology and Metabology, Graduate School of Medicine, Ehime University, Ehime, Japan

Yoichi Hiasa

Department of Gastroenterology and Metabology, Graduate School of Medicine, Ehime University, Ehime, Japan

Mamoru Aoto

Department of Physiology, Graduate School of Medicine, Ehime University, Ehime, Japan

Noriaki Mitsuda

Department of Physiology, Graduate School of Medicine, Ehime University, Ehime, Japan

Morikazu Onji

Department of Gastroenterology and Metabology, Graduate School of Medicine, Ehime University, Toon City, Ehime 791-0204, Japan, Phone: 81-089-960-5308, e-mail: onjimori@ m.ehme-u.ac.jp

ORIGINAL ARTICLE

SERUM ASPARATATE TRANSAMINASE PLATELET RATIO INDEX (APRI) IN PATIENTS WITH NON-ALCOHOLIC FATTY LIVER DISEASE IN BANGLADESH

Mir Fowaz Hossain[1], Mamun Al Mahtab[2], Sheikh Mohammad Fazle Akbar[3], Salimur Rahman[2]

ABSTRACT

Objective: *To correlate serum Aspartate transaminase (AST) and Platelet Ratio Index (APRI) with the degree of hepatic fibrosis in patients with non alcoholic fatty liver disease (NAFLD).*

Methodology: *This study was conducted on patients with NAFLD presenting at Bangabandhu Sheikh Mujib Medical University, Dhaka, Bangladesh, from July 2007 to June 2008. In all patients, platelet counts and levels of AST were measured in the sera. Percutaneous liver biopsy was done in these patients to assess the levels of hepatic fibrosis (HF). APRI was calculated by using the formula; AST×UNL×100/platelet count×10^9/L.*

Results: *Out of 30 patients, 28 had HF score of <2, while 2 had HF score of >2. However, high HF score was not associated with high AST. Based on platelet count, patients were divided into 2 groups; patients with platelet counts of <150,000/mm^3 and those with platelet counts of >150,000/mm^3. Sensitivity of APRI (cut off level 1.5) to diagnose significant fibrosis was 0%, specificity 96.4%, positive predictive value .0%, negative predictive value 93.1% and diagnostic accuracy 90.0%. On the other hand, when we considered APRI level of >1.5 as an indicator of significant fibrosis, one person was supposed to have hepatic fibrosis score of >2 from APRI value. But, liver histology of that person did not support hepatic fibrosis of >2.*

Conclusion: *APRI has no correlation with degree of hepatic fibrosis in patients with NAFLD and hence cannot be used as a non-invasive marker of fibrosis in patients with NAFLD in Bangladesh. However large scale studies are required to confirm these findings.*

Key Words: *Aspartate Transaminase Platelet Ratio Index, APRI, Non-Alcoholic Fatty Liver Disease (NAFLD), Hepatic Fibrosis.*

This article may be cited as: Hossain MF, Mahtab MA, Akbar SMF, Rahman S. Serum asparatate transaminase platelet count ratio index (APRI) in patients with non-alcoholic fatty liver disease in Bangladesh. Khyber Med Uinv J 2012;4(2):48-52

INTRODUCTION

Histopathological examination of the liver is an integral part of the diagnosis of patients with chronic liver disease (CLD). In addition, assessment of extent of liver damages and magnitudes of hepatic fibrosis allow proper designing of interventional strategies. Patients with chronic hepatitis with no or minimal fibrosis at presentation usually progress slowly and treatment may be delayed or withheld for the time being[1-3]. On the other hand, patients with significant hepatic fibrosis develop complications like liver cirrhosis, hepatic decompensation and hepatocellular carcinoma[4-6]. These patients should be provided with active therapeutic approaches, the guidelines for which have been provided by most of the professional organizations[7-8].

A well-performed liver biopsy and proper assessment of hepatic histology provides relevant information about extent of hepatic fibrosis in patients with CLD. However, this is not always possible in clinical settings. Also, there may be sampling error in liver biopsy because a small portion of liver tissues is used for evaluation[10,11]. In addition, facilities and trained manpower to accomplish liver biopsy are scanty in developing countries of the world that harbor the major bulk of patients with CLD.

These limitations have exposed the need of alternative and non-invasive methods of assessing hepatic fibrosis that are reliable, accurate, and acceptable to the

1 Department of Hepatology, Mymensingh Medical College, Mymensingh, Bangladesh
2 Department of Hepatology, Bangabandhu Sheikh Mujib Medical University, Dhaka, Bangladesh
3 Department of Medical Sciences, Toshiba General Hospital, Tokyo, Japan

Address for Correspondence:

Dr. Mamun-Al-Mahtab
Associate Professor
Department of Hepatology
Bangabandhu Sheikh Mujib Medical University
E-mail: shwapnil@agni.com

Date Submitted: October 28, 2011
Date Revised: May 22, 2012
Date Accepted: May 25, 2012

patient. Several serum markers such as serum hyaluronic acid, aspartate *transaminase (*aminotransferase)-to-alanine aminotransferase (ALT) ratio (AAR), aspartate *transaminase (*AST)-to-platelet ratio index (APRI), age-platelet count index (API) and many others[12-16]. Among these serum markers, the utility of APRI has been shown in patients with CLD. However, there is lack of consensus about its utility in CLDs due to different etiological agents. Some investigators have shown that APRI may be a good indicator showing various levels of fibrosis, whereas, the others could not confirm that. In general, the utility has been shown in chronic hepatitis C virus (HCV) infection with a moderate degree of accuracy. But, controversy remains about its utility in patients with chronic hepatitis B virus (HBV) infection[17-21]. Furthermore, little has been explored about clinical value of APRI in patients with autoimmune hepatitis as a biomarker of hepatic fibrosis.

Obesity and its associated conditions, including nonalcoholic fatty liver disease (NAFLD), have reached worldwide epidemic proportions. The pathological spectrum of NAFLD extends from simple hepatic steatosis to nonalcoholic steatohepatitis (NASH) to liver cirrhosis. In addition to liver-related complications, patients with NAFLD are more prone to develop insulin resistance, type 2 diabetes mellitus, and coronary heart disease[22-24]. Patients with NAFLD are also prone to develop severe complications. To accomplish a proper management guideline of NAFLD, assessment of extent of hepatic fibrosis is essential. In this context, there is paucity of information about the utility of APRI, a non-invasive marker of hepatic fibrosis, in patients with NAFLD. This study was aimed to correlate serum APRI with the degree of hepatic fibrosis in patients with NAFLD in Bangladesh.

METHODOLOGY

This was an open, non-randomized and consecutive observational type of clinical study. It was conducted at the Department of Hepatology, Bangabandhu Sheikh Mujib Medical University, Dhaka, Bangladesh in collaboration with the Department of Pathology of the same University. Thirty patients of NAFLD attending the Department of Hepatology of Bangabandhu Sheikh Mujib Medical University, Dhaka, Bangladesh from July 2007 to June 2008, were enrolled in the study. The diagnosis of NAFL was done from history of illness, body mass index, data of ultrasonography and those of liver function tests. The aims and objectives of the study along with its procedure, alternative diagnostic methods, risks and benefits of this study were explained to all patients in easily understandable local language and then written informed consents were obtained from the patients or their parents.

Patients with ultrasonographic evidence of fatty liver were included in this study. Patients with history of alcohol intake, chronic viral hepatitis (due to HBV and HCV), drug-induced chronic liver disease, patients in whom liver biopsy was contraindicated, and patients who were not willing to undergo liver biopsy were excluded from the study.

For liver biopsy, trucut biopsy needle was used. All aseptic precautions were maintained to avoid any complication. Local anesthetic agent was used. The biopsy needle was introduced through the right 8th or 9th intercostal space along the mid axillary line with the patient holding breath on expiration in quiet breathing. The direction of the needle was kept slightly posterior and cranial to avoid gall bladder injury. After biopsy procedure, the patient was kept lying on right side of the body for at least 2 hours. Pulse rate and blood pressure were recorded every 15 minutes for the first hour and then every 30 minutes for next 2 hours. Routine visits were paid at 4 and 8 hours. Patient was kept in bed rest for 24 hours. The biopsy material was sent for histopathology immersed in 10% formalin solution. Histopathological assessment of liver biopsy specimens was accomplished by two separate histopathologists and they were unaware of the diagnosis and clinical conditions of the patient. The assessment of hepatic fibrosis was done by the criteria of Kleiner et al[25].

Statistical analysis: Data were analyzed with the help of SPSS (Statistical package for social sciences) window's version 13 software. Statistical analysis was done using unpaired t-test and Chi square test. Statistical significance was set at $p<0.05$ and confidence interval was set at 95% level. All probability values quoted were 2-tailed.

RESULTS

The age of study population was 39.37±9.83 years (mean ± standard deviation). Out of all patients 16 (53.3%) were male and 14 (46.7%) were female (Table I). Housewives (40%) represented the commonest group among study population. They were followed by service holders (36.7%), students (16.7%), labourers (3.3%), and businessmen (3.3%).

Out of 30 patients 12 (40%), 16 (53.3%, and 2 (6.7%) patients had fibrosis of stage 1, 2, and 3, respectively (Table I). Taken together, mild to moderate fibrosis (fibrosis levels of 1 and 2) were detected in 28 (93.3%) patients, whereas, severe fibrosis (fibrosis level of 3) were seen in 2 (6.7%) patients. Regarding AST levels, 12 (40%), 9 (30%), and 9 (30%) patients had serum AST levels of <40 IU/ml, 40-50 IU/ml, and >50 IU/ml, respectively. Only 2 (6.7%) patients had fibrosis level 3; one (3.3%) of them

had AST level of <40 IU/ml and the other had AST level of >50 IU/ml.

Patients were divided in 2 groups on the basis of platelet count; platelet counts of <150,000/mm^3 and platelet count of >150,000/mm^3. In patients with mild and moderate fibrosis (fibrosis levels of 1 and 2), 3 of 28 patients had platelet count of <150000/mm^3 and 25 had platelet counts of >150,000/mm^3. In two patients with fibrosis levels of 3, both of the patients had platelet counts of >150,000/mm^3.

To develop more insights about this, we calculated APRI in all patients with NAFLD. The cut-off value of APRI for significant fibrosis was considered 0.5 (Table I). The APRI levels were <0.5 in 15 patients and were >0.5 in 15 patients. However, when these patients with APRI value of >0.5 were evaluated for hepatic fibrosis through assessment of liver biopsy specimens, 14/15 (93.3%) patients had only mild fibrosis. Only, one (6.7%) patient with APRI of >0.5 had significant fibrosis in liver biopsy specimen. In 15 cases, the levels of APRI were less than 0.5 indicating insignificant fibrosis by APRI assessment. One (6.7%) of these patients had significant fibrosis and 12 (80%) had mild fibrosis and 2 (13.3%) had moderate fibrosis by liver biopsy (Table I).

DEMOGRAPHIC PROFILES, HEPATIC FIBROSIS AND APRI IN PATIENTS WITH NAFLD

Number of Patients	30
Mean Age	39.4±9.6 years
Sex (male: female)	16:14
Liver histopathology	
Mild hepatic fibrosis (Fibrosis score 1)	12 (40%)
Moderate hepatic fibrosis (Fibrosis score 2)	16(53.3%)
Severe hepatic fibrosis (Fibrosis score 3)	2 (6.7%)
APRI<0.5	15 (50%)
Mild fibrosis	12
Moderate fibrosis	2
Severe fibrosis	1
APRI>0.5	
Extent of fibrosis by liver histology	15 (50%)
Mild fibrosis	14
Moderate fibrosis	0
Severe fibrosis	1

Table I

On the other hand when we considered APRI level >1.5 as a cut-off value for significant fibrosis, one patient with APRI>1.5 showed significant fibrosis, but that could not be confirmed by assessment of liver histopathology. Chi square test was done to know the association between variables (APRI and histopathological findings). Sensitivity of APRI (cut off level 1.5) to diagnose significant fibrosis was 0%, specificity 96.4%, positive predictive value .0%, negative predictive value 93.1% and histopathology accuracy 90.0%.

DISCUSSION

Proper assessment of liver histopathology, especially understandings about hepatic fibrosis is essential for designing the management of patients with CLDs. Although chronic hepatitis and its complications represented the major bulk of CLDs before one decade, recently NAFLD and their related complications appear to be major concern in clinics[22-24]. In fact, NAFLD and its complications have reached worldwide epidemic level. Thus, proper assessment of hepatic fibrosis represents a major challenge to clinical hepatologists.

To develop insights about utility of non invasive diagnostic approaches for NAFLD patients, we assessed the utility of APRI, a widely-used marker of hepatic fibrosis, for diagnosing patients with chronic liver diseases due to viral etiologies[17-21]. Our study showed that the implication of APRI would be limited, if any, in the diagnosis of hepatic fibrosis in NAFLD patients. The causes underlying this are not still clear. But, the pathogenic process of NAFLD and that of virus-induced chronic hepatitis seems to be different. Few studies have explored the comparative mechanism of fibrosis of chronic hepatitis due to viral etiology and NAFLD. It has been shown that a two-hit theory may be responsible for hepatic fibrosis in NAFLD patients,[23] whereas, alteration of hepatic microenvironment due to virus and their products may induce hepatic fibrosis in chronic viral hepatitis and their complications[26]. The role of hepatic stellate cells may have vital role in the process of fibrogenesis that is activated in different manner due to viral infection and in NAFLD[26].

The findings of this clinical study differs from that what have been reported by Yilmaz et al[27]. They showed that APRI seems to be a potentially good marker of non invasive diagnosis of chronic hepatitis C and NAFLD, but they clearly marked that APRI has limited role in diagnosis of chronic hepatitis B. However, our study supports what that have been reported by Adams et al[28]. They mentioned that any simple serum marker may not be a good predictor of hepatic fibrosis in NAFLD. They also suggested that complex invasive fibrosis model would be required to have an accurate diagnosis of

NAFLD. Thus, emerging evidences have been accumulated to compare the utility of different non invasive markers of diagnosis of chronic liver diseases. Further studies would be required to develop more insights in this regard.

Indeed, there are some limitations of this study that have been compiled in Bangladesh. The sample size is relatively small. We could only enroll 30 patients with NAFLD. The small sample size was mainly attributable to the fact that only those patients who provided consent for liver biopsy were enrolled in this study. In fact, most of the patients in developing countries are reluctant to accept an invasive test like liver biopsy. The next, we enrolled only patients with NAFLD. A comparative analysis of utility of APRI in NAFLD patients and patients with CLDs due to viral etiology would shed more insights about the utility of APRI as a non invasive marker in our population.

Although the outcome of this study is a negative one, but it shows the utility of non invasive marker of hepatic fibrosis should be analyzed cautiously in patients with liver diseases with different etiologies. Also, the study should be conducted in different races and socio-economic groups to validate the real implications of these markers. As this is the first study about utility of APRI in Bangladesh, this study would initiate more studies of this nature with large sample size in future.

REFERENCES

1. Liaw YF, Chu CM. Hepatitis B virus infection. Lancet 2009 ; 373: 582-92.
2. Lok AS, McMahon BJ. Chronic hepatitis B. Hepatology 2007; 45: 507-39.
3. Zoulim F, Perrillo R. Hepatitis B: reflections on the current approach to antiviral therapy. J Hepatol 2008; 48 Suppl 1: S2-19.
4. Liaw YF. Natural history of chronic hepatitis B virus infection and long-term outcome under treatment. Liver Int 2009; 29 Suppl 1: 100-7.
5. Camma C, Giunta M, Andreone P, Craxi A. Interferon and prevention of hepatocellular carcinoma in viral cirrhosis: an evidence-based approach. J Hepatol 2001; 34: 593-602.
6. Chien RN. On-treatment monitoring of chronic hepatitis B virus infection: An Asian-Pacific perspective. J Gastroenterol Hepatol 2010; 25: 852-7.
7. Lok AS and McMahon BJ. AASLD Guidelines Chronic hepatitis B; Update 2009; Hepatology 2009; 50: 1-36.
8. European Association for the Study of the Liver: EASL clinical practice guidelines; Management of chronic hepatitis B. J Hepatol. 2009; 50: 227-42.
9. Liaw YF, Leung N, Guan R, Lau GK, Merican I, McCaughan G, et al. Asian-Pacific consensus statement on the management of chronic hepatitis B: a 2008 update. Hepatol Int 2008; 22: 262-83.
10. Bedossa P, Dargere D, Paradis V. Sampling variability of liver fibrosis in chronic hepatitis C. Hepatology 2003; 38: 1449-57.
11. Colleredo G, Guido M, Sonzogni A, Leandro G. Impact of liver biopsy size on histological evaluation of chronic viral hepatitis: the smaller the sample, the milder the disease. J Hepatol 2003; 39: 239-44.
12. Sheth SG, Flamm SI, Gordon SD, Chopra S. AST/ALT ratio predicts cirrhosis in patients with chronic hepatitis C virus infections. Am J Gastroenterol 1998; 93: 44-8.
13. Loaeza-del-Castillo A, Paz-Pineda F, Oviedo-Cárdenas E, Sánchez-Avila F, Vargas-Voráckova F. AST to platelet ratio index (APRI) for the noninvasive evaluation of liver fibrosis. Ann Hepatol 2008; 7: 350-7.
14. Fraser JRE, Laurent TC, Laurent UB. Hyaluronan: Its nature, distribution, functions and turnover. J Intern Med 1997; 242: 27-33.
15. Wai CT, Greenson JK, Fontana RJ,Marrero JA. Noninvasive models for predicting histology in patients with chronic hepatitis B. Liver Int 2006; 26: 666-72.
16. Wai CT, Greenson JK, Fontana RJ, Kalbfleisch JD, Marrero JA, 'Conjeevaram HS, et al. A simple noninvasive index can predict both significant fibrosis and cirrhosis in patients with chronic hepatitis C'. Hepatology 2003; 38, 518-26.
17. Lin ZH, Xin YN, Dong QJ, Wang Q, Jiang XJ, Zhan SH, et al. Performance of the aspartate aminotransferase-to-platelet ratio index for the staging of hepatitis C-related fibrosis: an updated meta-analysis. Hepatology 2011; 53: 726-36.
18. Kim BK, Kim SA, Park YN, Cheong JY, Kim HS, Park JY, et al. Non-invasive models to predict liver cirrhosis in patients with chronic hepatitis B. Liver Int 2007; 27(7): 969-76.
19. Zeng MD, Lu LG, Mao YM, Qiu DK, Li JQ, Wan MB, et al. Prediction of significant fibrosis in HBeAg-Positive patients with Chronic Hepatitis B by a noninvasive model. Hepatology 2005; 42: 1437-45.
20. Alex Yui Hui, Joseph Jao Sung. Identification of chronic hepatitis B patients without significant liver fibrosis by a simple noninvasive predictive model. Am J Gastroenterol 2005; 100: 616-23.
21. Obara N, Ueno Y, Fukushima K, Nakagome Y, Kakazu E, Kimura O, et al. Transient elastography for measurement of liver stiffness measurement can detect early significant hepatic fibrosis in Japanese patients with viral and nonviral liver diseases. J Gastroenterol 2008; 43: 720-8.
22. Tordjman J, Guerre-Millo M, Clément K. Adipose tissue inflammation and liver pathology in human obesity. Diabetes Metab 2008; 34: 658-63.
23. Day CP, James OF. Steatohepatitis: A tale of two "hits"? Gastroenterol 1998; 114: 842-5.

24. de Luca C, Olefsky JM. Inflammation and insulin resistance. FEBS Lett 2008; 582: 97-105.

25. Kleiner DE, Brunt EM, Van Natta ML. 'Nonalcoholic Steatohepatitis Clinical Research Network. Design and validation of a histologic scoring system for NAFLD'. Hepatol 2005; 41: 1313-21.

26. Chakraborty JB, Oakley F, Walsh MJ. Mechanisms and biomarkers of apoptosis in liver disease and fibrosis. Int J Hepatol 2012; 2012: 648915. Epub 2012 Apr 9.

27. Yilmaz Y, Yonal O, Kurt R, Bayrak M, Aktas B, Ozdogan O. Noninvasive assessment of liver fibrosis with the aspartate transaminase to platelet ratio index (APRI): Usefulness in patients with chronic liver disease: APRI in chronic liver disease. Hepat Mon 2011; 11: 103-6.

28. Adams LA, George J, Bugianesi E, Rossi E, De Boer WB, van der Poorten D, et al. Complex non-invasive fibrosis models are more accurate than simple models in non-alcoholic fatty liver disease. J Gastroenterol Hepatol 2011; 26: 1536-43.

AUTHOR'S CONTRIBUTION

Following authors have made substantial contributions to the manuscript as under:

FH: Conception and design, Analysis and interpretation of data.

MAH: Analysis of data, Critical revision of manuscript

SMFA: Drafting the manuscript.

SR: Acquisition of data

CONFLICT OF INTEREST

Authors declare no conflict of interest

GRANT SUPPORT AND FINANCIAL DISCLOSURE

NONE DECLARED

HEPATOLOGY
Official Journal of the American Association for the Study of Liver Diseases

Discrete Nature of EpCAM$^+$ and CD90$^+$ Cancer Stem Cells in Human Hepatocellular Carcinoma

Taro Yamashita,[1] Masao Honda,[1] Yasunari Nakamoto,[1] Masayo Baba,[1] Kouki Nio,[1] Yasumasa Hara,[1] Sha Sha Zeng,[1] Takehiro Hayashi,[1] Mitsumasa Kondo,[1] Hajime Takatori,[1] Tatsuya Yamashita,[1] Eishiro Mizukoshi,[1] Hiroko Ikeda,[1] Yoh Zen,[1] Hiroyuki Takamura,[1] Xin Wei Wang,[2] and Shuichi Kaneko[1]

Recent evidence suggests that hepatocellular carcinoma (HCC) is organized by a subset of cells with stem cell features (cancer stem cells; CSCs). CSCs are considered a pivotal target for the eradication of cancer, and liver CSCs have been identified by the use of various stem cell markers. However, little information is known about the expression patterns and characteristics of marker-positive CSCs, hampering the development of personalized CSC-targeted therapy. Here, we show that CSC markers EpCAM and CD90 are independently expressed in liver cancer. In primary HCC, EpCAM$^+$ and CD90$^+$ cells resided distinctively, and gene-expression analysis of sorted cells suggested that EpCAM$^+$ cells had features of epithelial cells, whereas CD90$^+$ cells had those of vascular endothelial cells. Clinicopathological analysis indicated that the presence of EpCAM$^+$ cells was associated with poorly differentiated morphology and high serum alpha-fetoprotein (AFP), whereas the presence of CD90$^+$ cells was associated with a high incidence of distant organ metastasis. Serial xenotransplantation of EpCAM$^+$/CD90$^+$ cells from primary HCCs in immune-deficient mice revealed rapid growth of EpCAM$^+$ cells in the subcutaneous lesion and a highly metastatic capacity of CD90$^+$ cells in the lung. In cell lines, CD90$^+$ cells showed abundant expression of c-Kit and *in vitro* chemosensitivity to imatinib mesylate. Furthermore, CD90$^+$ cells enhanced the motility of EpCAM$^+$ cells when cocultured *in vitro* through the activation of transforming growth factor beta (TGF-β) signaling, whereas imatinib mesylate suppressed *TGFB1* expression in CD90$^+$ cells as well as CD90$^+$ cell-induced motility of EpCAM$^+$ cells. *Conclusion*: Our data suggest the discrete nature and potential interaction of EpCAM$^+$ and CD90$^+$ CSCs with specific gene-expression patterns and chemosensitivity to molecular targeted therapy. The presence of distinct CSCs may determine the clinical outcome of HCC. (HEPATOLOGY 2012;00:000–000)

The cancer stem cell (CSC) hypothesis, which suggests that a subset of cells bearing stem-cell–like features is indispensable for tumor development, has recently been put forward subsequent to advances in molecular and stem cell biology. Liver cancer, including hepatocellular carcinoma (HCC), is a leading cause of cancer death worldwide.[1] Recent studies have shown the existence of CSCs in liver cancer cell lines and primary HCC specimens using various stem cell markers.[2-7] Independently, we have identified novel HCC subtypes defined by the hepatic stem/progenitor cell markers,

Abbreviations: 5-FU, fluorouracil; Abs, antibodies; AFP, alpha-fetoprotein; CK-19, cytokeratin-19; CSC, cancer stem cell; DNs, dysplastic nodules; EMT, epithelial mesenchymal transition; EpCAM; epithelial cell adhesion molecule; FACS, fluorescent-activated cell sorting; HBV, hepatitis B virus; HCC, hepatocellular carcinoma; HCV, hepatitis C virus; HSCs, hepatic stem cells; IF, immunofluorescence; IHC, immunohistochemistry; IR, immunoreactivity; MDS, multidimensional scaling; NBNC, non-B, non-C hepatitis; NOD/SCID, nonobese diabetic, severe combined immunodeficient; NT, nontumor; OV-1, ovalbumin 1; qPCR, quantitative real-time polymerase chain reaction; SC, subcutaneous; Smad3, Mothers against decapentaplegic homolog 3; TECs, tumor epithelial cells; TGF-β, transforming growth factor beta; T/N, tumor/nontumor; VECs, vascular endothelial cells; VM, vasculogenic mimicry; VEGFR, vascular endothelial growth factor receptor.

From the [1]Liver Center, Kanazawa University Hospital, Kanazawa, Ishikawa, Japan; and [2]Laboratory of Human Carcinogenesis, Center for Cancer Research, National Cancer Institute, Bethesda, MD.

Received July 9, 2012; revised October 22, 2012; accepted November 6, 2012.

This study was supported by a Grant-in-Aid from the Ministry of Education, Culture, Sports, Science, and Technology of Japan (23590967), a grant from the Japanese Society of Gastroenterology, a grant from the Ministry of Health, Labor, and Welfare, and a grant from the National Cancer Center Research and Development Fund (23-B-5) of Japan. X.W.W. is supported by the Intramural Research Program of the Center for Cancer Research, U.S. National Cancer Institute.

epithelial cell adhesion molecule (EpCAM) and alpha-fetoprotein (AFP), which correlate with distinct gene-expression signatures and prognosis.[8,9] EpCAM$^+$ HCC cells isolated from primary HCC and cell lines show CSC features, including tumorigenicity, invasiveness, and resistance to fluorouracil (5-FU).[10] Similarly, other groups have shown that CD133$^+$, CD90$^+$, and CD13$^+$ HCC cells are also CSCs, and that EpCAM, CD90, and CD133 are the only markers confirmed to enrich CSCs from primary HCCs thus far.[3-5,10]

Although EpCAM$^+$, CD90$^+$, and CD133$^+$ cells show CSC features, such as high tumorigenicity, an invasive nature, and resistance to chemo- and radiation therapy, it remains unclear whether these cells represent an identical HCC population and whether they share similar or distinct characteristics. In this study, we used fluorescent-activated cell sorting (FACS), microarray, and immunohistochemistry (IHC) techniques to investigate the expression patterns of the representative liver CSC markers CD133, CD90, and EpCAM in a total of 340 HCC cases and 7 cases of mesenchymal liver tumors. We further explored gene- and protein-expression patterns as well as tumorigenic capacity of sorted cells isolated from 15 primary HCCs and 7 liver cancer cell lines in an attempt to identify the molecular portraits of each cell type.

Materials and Methods

Clinical Specimens. HCC samples were obtained with informed consent from patients who had undergone radical resection at the Liver Center in Kanazawa University Hospital (Kanazawa, Japan), and tissue acquisition procedures were approved by the ethics committee of Kanazawa University. A total of 102 formalin-fixed and paraffin-embedded HCC samples, obtained from 2001 to 2007, were used for IHC analyses. Fifteen fresh HCC samples were obtained between 2008 and 2012 from surgically resected specimens and an autopsy specimen and were used immediately to prepare single-cell suspensions and xenotransplantation (Table 1). Seven hepatic stromal tumors (three cavernous hemangioma, two hemangioendothelioma, and two angiomyolipoma) were formalin fixed and paraffin embedded and used for IHC analyses.

Table 1. Clinicopathological Characteristics of HCC Cases Used for Xenotransplantation

ID	Age/ Sex	Etiology	Tumor Size (cm)	Histological Grade	AFP (ng/mL)	DCP (IU/mL)
P1	77/M	Alcohol	12.0	Moderate	198	322
P2	61/F	NBNC	11.0	Moderate	12	3,291
P3	66/M	NBNC	2.2	Moderate	13	45
P4	65/M	HCV	4.2	Poor	13,700	25,977
P5	52/M	HBV	6.0	Moderate	29,830	1,177
P6	60/M	HCV	2.7	Poor	249	185
P7	79/F	HBV	4.0	Poor	46,410	384
P8	77/F	NBNC	5.5	Moderate	17,590	562
P9	71/M	Alcohol	7.0	Poor	3,814	607
P10	51/M	HBV	2.2	Well	<10	21
P11	71/M	Alcohol	2.1	Well	<10	11
P12	60/M	HBV	10.8	Poor	323	2,359
P13	66/M	HCV	2.8	Moderate	11	29
P14	71/M	HCV	7.2	Moderate	235,700	375,080
P15	75/M	HBV	5.5	Poor	<10	97

Abbreviation: DCP, des-gamma-carboxy prothrombin.

Additional details of experimental procedures are available in the Supporting Information.

Results

EpCAM, CD133, and CD90 Expression in HCC. We first evaluated the frequencies of three representative CSC markers (EpCAM$^+$, CD90$^+$, and CD133$^+$ cells) in 12 fresh primary HCC cases surgically resected by FACS (representative data shown in Fig. 1A). Clinicopathological characteristics of primary HCC cases are shown in Table 1. We noted that frequency of EpCAM$^+$, CD90$^+$, and CD133$^+$ cells varied between individuals. Abundant CD90$^+$ (7.0%), but almost no EpCAM$^+$, cells (0.06%, comparable to the isotype control) were detected in P2, whereas few CD90$^+$ (0.6%), but abundant EpCAM$^+$, cells (17.5%) were detected in P4. Very small populations of EpCAM$^+$ (0.09%), CD90$^+$ (0.04%), and CD133$^+$ cells (0.05%) were found in P12, but they were almost nonexistent in P8, except for CD90$^+$ cells (0.08%) (Fig. 1A). We further evaluated the expression of EpCAM, CD90, and CD133 in xenografts obtained from surgically resected samples (P13 and P15) and an autopsy sample (P14). As a whole, compared to the isotype control, 7 of 15 HCCs contained definite EpCAM$^+$ cells (46.7%), whereas only 3 HCCs

Address reprint requests to: Taro Yamashita, M.D., Ph.D., Department of General Medicine, Kanazawa University Hospital, 13-1 Takara-Machi, Kanazawa, Ishikawa 920-8641, Japan. E-mail: taroy@m-kanazawa.jp; fax: +81-76-234-4250.

View this article online at wileyonlinelibrary.com.
DOI 10.1002/hep.26168
Potential conflict of interest: Nothing to report.
Additional Supporting Information may be found in the online version of this article.

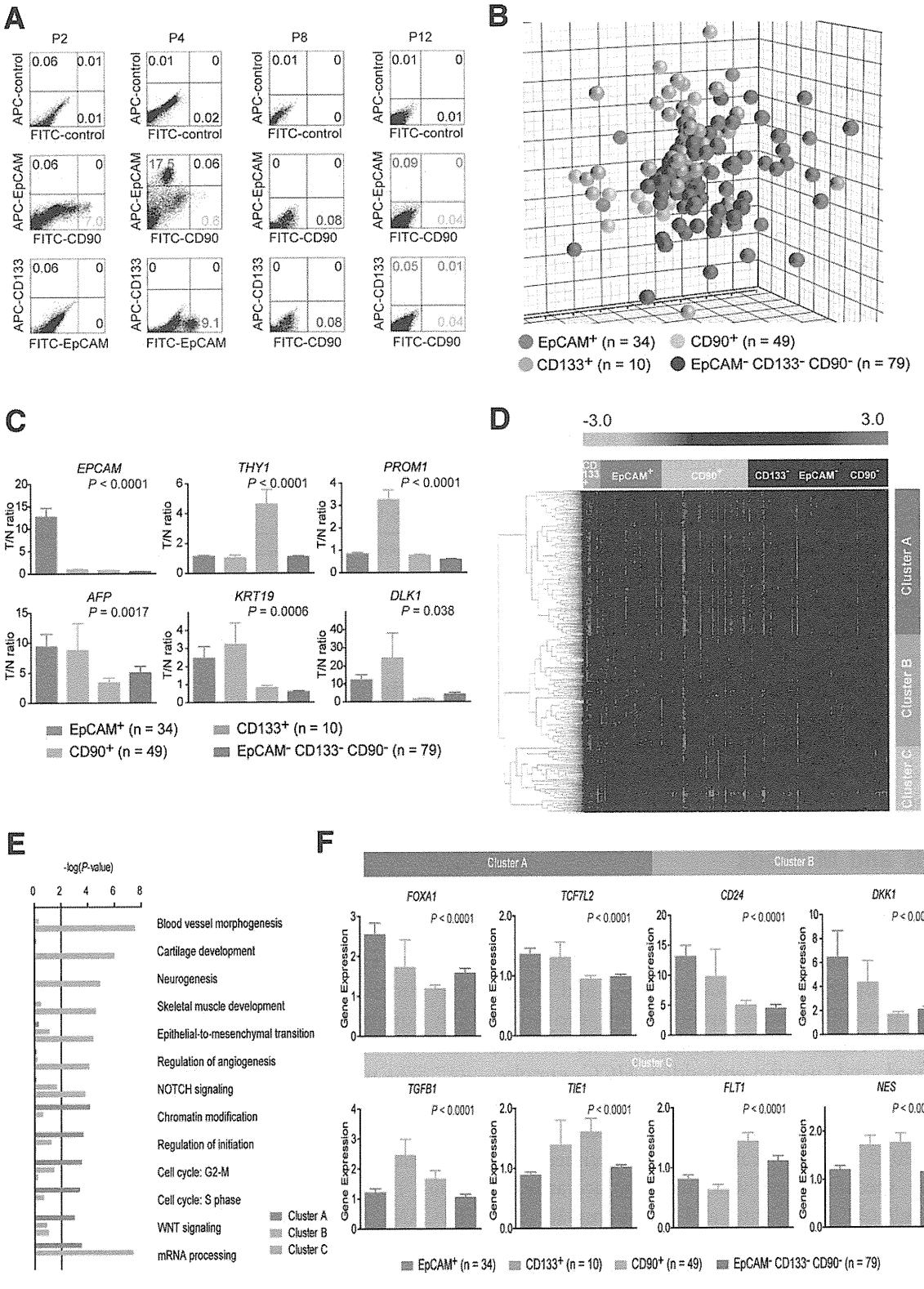

Fig. 1. Gene-expression profiles of CSC marker-positive HCCs. (A) FACS analysis of primary HCCs stained with fluorescent-labeled Abs against EpCAM, CD90, or CD133. (B) Multidimensional scaling analysis of 172 HCC cases characterized by the expression patterns of EpCAM, CD133, and CD90. Red, $EpCAM^+$ $CD90^-$ $CD133^-$ (n = 34); orange, $EpCAM^-$ $CD90^-$ $CD133^+$ (n = 10); light blue, $EpCAM^-$ $CD90^+$ $CD133^-$ (n = 49); blue, $EpCAM^-$ $CD90^-$ $CD133^-$ (n = 79). HCC specimens were clustered in specific groups with statistical significance ($P < 0.001$). (C) Expression patterns of well-known hepatic stem/progenitor markers in each HCC subtype, as analyzed by microarray. Red bar, $EpCAM^+$; orange bar, $CD133^+$; light blue bar, $CD90^+$; blue bar, $EpCAM^-$ $CD90^-$ $CD133^-$. (D) Hierarchical cluster analysis based on 1,561 EpCAM/CD90/CD133-coregulated genes in 172 HCC cases. Each cell in the matrix represents the expression level of a gene in an individual sample. Red and green cells depict high and low expression levels, respectively, as indicated by the scale bar. (E) Pathway analysis of EpCAM/CD90/CD133-coregulated genes. Canonical signaling pathways activated in cluster A (red bar), cluster B (orange bar), or cluster C (light blue bar) with statistical significance ($P < 0.01$) are shown. (F) Expression patterns of representative genes differentially expressed in EpCAM/CD90/CD133 HCC subtypes. Red bar, $EpCAM^+$; orange bar, $CD133^+$; light blue bar, $CD90^+$; blue bar, $EpCAM^-$ $CD133^-$ $CD90^-$.

Table 2. Tumorigenic Capacity of Unsorted, EpCAM$^+$, EpCAM$^-$, CD90$^+$, and CD90$^-$ Cells From Primary HCCs and Xenografts

Sample	CD133 (%)	CD90 (%)	EpCAM (%)	Cell Surface Marker	Number of Cells	Tumor Formation 2M	Tumor Formation 3M
P1	0	3.1	0	Unsorted	1×10^7	0/5	0/5
				CD90$^+$	1×10^5	0/5	0/5
				CD90$^-$	1×10^5	0/5	0/5
P2	0.06	7.0	0.06	Unsorted	1×10^7	0/5	0/5
				CD90$^+$	1×10^5	0/5	0/5
				CD90$^-$	1×10^5	0/5	0/5
P3	0	1.3	0	Unsorted	1×10^6	0/2	0/2
				CD90$^+$	1×10^4	0/4	0/4
				CD90$^-$	1×10^4	0/4	0/4
P4	0	0.6	17.5	Unsorted	1×10^6	3/4	4/4
				EpCAM$^+$	1×10^3	0/3	2/3
					1×10^4	3/4	4/4
					1×10^5	3/3	3/3
				CD90$^+$	1×10^3	0/3	0/3
					1×10^4	0/4	0/4
					1×10^5	0/3	0/3
				EpCAM$^-$ CD90$^-$	1×10^3	0/3	0/3
					1×10^4	0/4	0/4
					1×10^5	0/3	0/3
P5	0	0.8	29.7	Unsorted	1×10^6	0/5	0/5
				EpCAM$^+$	1×10^5	0/5	0/5
				CD90$^+$	1×10^5	0/5	0/5
				EpCAM$^-$ CD90$^-$	1×10^5	0/5	0/5
P6	0	0.7	0	Unsorted	1×10^6	0/2	0/2
				CD90$^+$	1×10^4	0/4	0/4
				CD90$^-$	1×10^4	0/4	0/4
P7	1.38	4.5	4.4	Unsorted	1×10^6	2/2	2/2
				EpCAM$^+$	2×10^2	0/3	0/3
					1×10^3	0/3	1/3
					1×10^4	2/4	4/4
				CD90$^+$	2×10^2	0/3	0/3
					1×10^3	0/3	0/3
					1×10^4	0/4	0/4
				EpCAM$^-$ CD90$^-$	1×10^3	0/3	0/3
					1×10^4	0/3	0/3
					1×10^5	0/4	0/4
P8	0	0.08	0	Unsorted	1×10^5	0/4	0/4
				CD90$^+$	1×10^3	0/3	0/3
				CD90$^-$	1×10^5	0/3	0/3
P9	0	0.26	0	Unsorted	1×10^5	0/4	0/4
				CD90$^+$	1×10^3	0/3	0/3
				CD90$^-$	1×10^5	0/3	0/3
P10	0	0.78	0	Unsorted	1×10^4	0/4	0/4
				CD90$^+$	1×10^3	0/3	0/3
				CD90$^-$	1×10^4	0/3	0/3
P11	0	0.1	1.54	Unsorted	5×10^4	0/2	0/2
				EpCAM$^+$	1×10^3	0/3	0/3
				CD90$^+$	1×10^3	0/3	0/3
				EpCAM$^-$ CD90$^-$	1×10^4	0/3	0/3
P12	0.06	0.05	0.09	Unsorted	1×10^5	0/3	3/3
				CD90$^+$	1×10^3	0/4	1/4
				CD90$^-$	1×10^3	0/4	1/4
					1×10^4	0/3	3/3
P13	0	0.03	67.7	EpCAM$^+$	5×10^5	4/4	NA
					5×10^4	3/3	NA
					5×10^3	3/3	NA
				EpCAM$^-$	5×10^5	0/4	NA
					5×10^4	0/3	NA
					5×10^3	0/3	NA
P14	24.0	0.06	3.1	EpCAM$^+$	5×10^3	4/5	NA
				EpCAM$^-$	5×10^3	2/5	NA
P15	0	2.45	0	CD90$^+$	5×10^4	3/4	NA
					5×10^3	1/3	NA
					5×10^2	1/3	NA
				CD90$^-$	5×10^4	2/4	NA
					5×10^3	1/3	NA
					5×10^2	0/3	NA

NA, not available.

contained definite CD133$^+$ cells (20%) (Table 2). CD90$^+$ cells were detected at variable frequencies in all 15 HCCs analyzed.

To explore the status of these CSC marker-positive cells in HCC in a large cohort, we utilized oligo-DNA microarray data from 238 HCC cases (GEO accession no.: GSE5975) to evaluate the expression of *EPCAM* (encoding EpCAM and CD326), *THY1* (encoding CD90), and *PROM1* (encoding CD133) in whole HCC tissues and nontumor (NT) tissues. Because previous studies demonstrated that CD133$^+$ and CD90$^+$ cells were detected at low frequency (~13.6% by CD133 staining and ~6.2% by CD90 staining) in HCC, but were almost nonexistent in NT liver (4, 5),[4,5] we utilized tumor/nontumor (T/N) gene-expression ratios to detect the existence of marker-positive CSCs in tumor. Accordingly, we showed that a 2-fold cutoff of T/N ratios of *EPCAM* successfully stratifies HCC samples with EpCAM$^+$ liver CSCs.[9,10]

A total of 95 (39.9%), 110 (46.2%), and 31 (13.0%) of the 238 HCC cases were thus regarded as EpCAM$^+$, CD90$^+$, and CD133$^+$ HCCs (T/N ratios: $\geq$2.0), respectively. As observed in the FACS data described above, we detected coexpression of EpCAM and CD90 in 45 HCCs (18.9%), EpCAM and CD133 in five HCCs (2%), CD90 and CD133 in five HCCs (2%), and EpCAM, CD90, and CD133 in 11 HCCs (4.6%). To clarify the characteristics of gene-expression signatures specific to stem cell marker expression status, we selected 172 HCC cases expressing a single CSC marker (34 EpCAM$^+$ CD90$^-$ CD133$^-$, 49 EpCAM$^-$ CD90$^+$ CD133$^-$, and 10 EpCAM$^-$ CD90$^-$ CD133$^+$) or all marker-negative HCCs (79 EpCAM$^-$ CD90$^-$ CD133$^-$). A class-comparison analysis with

univariate F tests and a global permutation test (×10,000) yielded a total of 1,561 differentially expressed genes. Multidimensional scaling (MDS) analysis using this gene set indicated that HCC specimens were clustered in specific groups with statistical significance ($P < 0.001$). Close examination of MDS plots revealed three major HCC subtype clusters: all marker-negative HCCs (blue spheres); EpCAM single-positive HCCs (red spheres); and CD90 single-positive HCCs (light blue spheres). $CD133^+$ HCCs (orange spheres) were rare, relatively scattered, and not clustered (Fig. 1B).

We examined the expression of representative hepatic stem/progenitor cell markers *AFP*, *KRT19*, and *DLK1* in HCCs with regard to the gene-expression status of each CSC marker (Fig. 1C). All three markers were up-regulated in $EpCAM^+$ and $CD133^+$ HCCs, compared with all marker-negative HCCs, consistent with previous findings.[10,11] However, we found no significant overexpression of *AFP*, *KRT19*, and *DLK1* in $CD90^+$ and all marker-negative HCCs.

Hierarchical cluster analyses revealed three main gene clusters that were up-regulated in $EpCAM^+$ HCCs (cluster A, 706 genes), $EpCAM^+$ or $CD133^+$ HCCs (cluster B, 530 genes), and $CD90^+$ or $CD133^+$ HCCs (cluster C, 325 genes) (Fig. 1D). Pathway analysis indicated that the enriched genes in cluster A (red bar) were associated with chromatin modification, cell-cycle regulation, and Wnt/β-catenin signaling (Fig. 1E). Genes associated with messenger RNA processing were enriched in clusters A (red bar) and B (orange bar). Surprisingly, genes in cluster C were significantly associated with pathways involved in blood-vessel morphogenesis, angiogenesis, neurogenesis, and epithelial mesenchymal transition (EMT) (light blue bar). Close examination of genes in each cluster suggested that known hepatic transcription factors (*FOXA1*), Wnt regulators (*TCF7L2* and *DKK1*), and a hepatic stem cell marker (*CD24*) were dominantly up-regulated in $EpCAM^+$ and $CD133^+$ HCCs (Fig. 1F). By contrast, genes associated with blood-vessel morphogenesis (*TIE1* and *FLT1*), EMT (*TGFB1*), and neurogenesis (*NES*) were activated dominantly in $CD90^+$ HCCs and $CD133^+$ HCCs.

$CD90^+$ HCC Cells Share Features With Mesenchymal Vascular Endothelial Cells. Because $CD133^+$ HCCs were relatively rare and constituted only 13% (microarray cohort) to 20% (FACS cohort) of all HCC samples analyzed, we focused on the characterization of EpCAM and CD90. To clarify the cell identity of $EpCAM^+$ or $CD90^+$ cells in primary HCCs, we performed IHC analysis of 18 needle-biopsy specimens of premalignant dysplastic nodules (DNs), 102 surgically resected HCCs, and corresponding NT liver tissues. When examining the expression of EpCAM and CD90 in cirrhotic liver tissue by double-color IHC analysis, we found that $EpCAM^+$ cells and $CD90^+$ cells were distinctively located and not colocalized (Supporting Fig. 1A). Immunoreactivity (IR) to anti-CD90 antibodies (Abs) was detected in vascular endothelial cells (VECs), inflammatory cells, fibroblasts, and neurons, but not in hepatocytes or cholangiocytes, in the cirrhotic liver (Supporting Fig. 1B, panels a,b). IR to anti-EpCAM Abs was detected in hepatic progenitors adjacent to the periportal area and bile duct epithelial cells in liver cirrhosis (Supporting Fig. 1B, panels c,d).

IR to anti-EpCAM Abs was detected in 37 of 102 surgically resected HCCs (Fig. 2A, panel b), but not in 18 DNs (Fig. 2A, panel a). By contrast, no tumor epithelial cells (TECs) showing IR to anti-CD90 Abs were found in any of the 18 DNs or 102 HCCs examined (Fig. 2A, panels c,d). However, we identified $CD90^+$ cells that were morphologically similar to VECs or fibroblasts within the tumor nodule in 37 of the 102 surgically resected HCC tissues (≥5% positive staining in a given area). IR to anti-CD90 Abs was also detected in hepatic mesenchymal tumors (Supporting Fig. 1C, panels a-c), indicating that CD90 is also a marker of liver stromal tumors.

Double-color IHC and immunofluorescence (IF) analysis confirmed the distinct expression of EpCAM and CD90 in HCC (Fig. 2B), consistent with the FACS data (Fig. 1A). Quantitative real-time polymerase chain reaction (qPCR) analysis of sorted $EpCAM^+$, $CD90^+$, and $EpCAM^-$ $CD90^-$ cells after $CD45^+$ cell depletion indicated that the hepatic stem/progenitor markers, *AFP* and *KRT19*, were up-regulated in $EpCAM^+$ cells (red bar), whereas the mesenchymal markers, *KIT* and *FLT1*, were up-regulated in $CD90^+$ cells (orange bar), compared with $EpCAM^-$ $CD90^-$ cells (blue bar) (Fig. 2C). The hepatocyte marker, *CYP3A4*, was down-regulated in $EpCAM^+$ cells and not detected in $CD90^+$ cells, compared with $EpCAM^-$ $CD90^-$ cells. *POU5F1* and *BMI1* were equally up-regulated in both $EpCAM^+$ and $CD90^+$ cells, compared with $EpCAM^-$ $CD90^-$ cells.

EpCAM and CD90 were independently and distinctively expressed in different cellular lineages, so we evaluated the staining of EpCAM and CD90 separately and analyzed the clinicopathological characteristics of surgically resected HCC cases. HCCs were regarded marker positive if ≥5% positive staining was detected in a given area. The existence of $EpCAM^+$

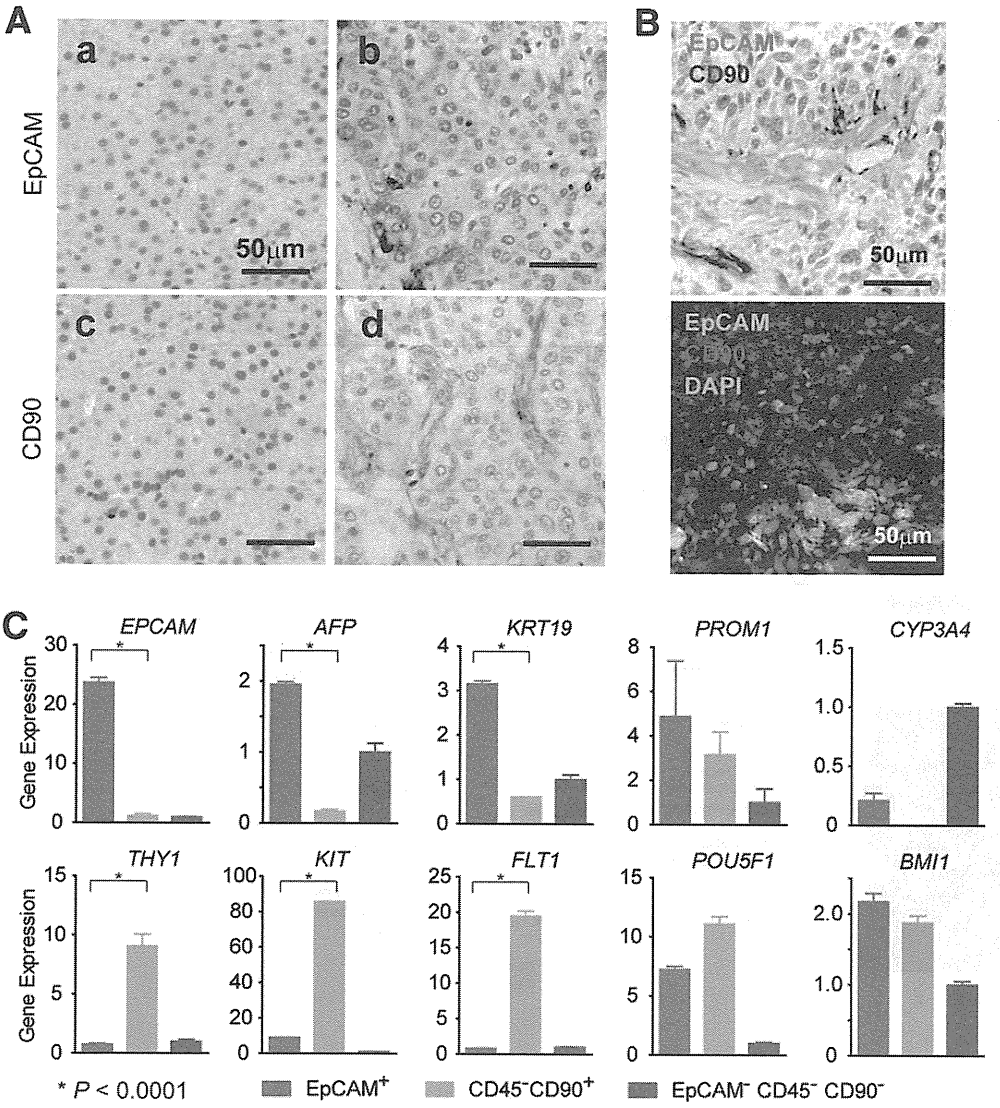

Fig. 2. Distinct EpCAM$^+$ and CD90$^+$ cell populations in HCC. (A) Representative images of EpCAM and CD90 staining in dysplastic nodule (panels a,c) and HCC (panels b,d) by IHC analysis (scale bar, 50 μm). EpCAM (panels a,b) and CD90 (panels c,d) immunostaining is depicted. (B) Upper panel: representative images of EpCAM (red) and CD90 (brown) double staining in HCC by IHC (scale bar, 50 μm). Lower panel: representative images of EpCAM (green) and CD90 (red) staining with 4'6-diamidino-phenylindole (DAPI) (blue) in HCC by IF (scale bar, 50 μm). (C) qPCR analysis of sorted EpCAM$^+$ (red bar), CD90$^+$ (orange bar), or EpCAM$^-$ CD90$^-$ (blue bar) derived from a representative primary HCC. Experiments were performed in triplicate, and data are shown as mean ± standard error of the mean.

cells (≥5%) was characterized by poorly differentiated morphology and high serum AFP values with a tendency for portal vein invasion, whereas the existence of CD90$^+$ cells (≥5%) was associated with poorly differentiated morphology and a tendency for large tumor size (Supporting Tables 2 and 3). Notably, the existence of CD90$^+$ cells was associated with a high incidence of distant organ metastasis, including lung, bone, and adrenal gland, within 2 years after surgery, whereas EpCAM$^+$ cell abundance appeared unrelated to distant organ metastasis.

We evaluated the characteristics of EpCAM$^+$ or CD90$^+$ cells in seven representative HCC cell lines. Morphologically, all EpCAM$^+$ cell lines (HuH1, HuH7, and Hep3B) showed a polygonal, epithelial cell shape, whereas three of four CD90$^+$ cell lines (HLE, HLF, and SK-Hep-1) showed a spindle cell shape (Fig. 3A). EpCAM$^+$ cells were detected in 11.5%, 57.7%, and 99.6% of sorted HuH1, HuH7, and Hep3B cells, respectively. A small CD90$^+$ cell population (0.66%) was observed in PLC/PRL/5, whereas 91.3%, 10.8%, and 59.0% of CD90$^+$ cells were detected in HLE, HLF, and SK-Hep-1, respectively. Compared with primary HCCs, only EpCAM$^+$ or CD90$^+$ cells were detected in liver cancer cell lines under normal culture conditions (Fig. 3B), suggesting that these cell lines contain a relatively pure cell population most likely obtained by clonal selection through the establishment process.

A class-comparison analysis with univariate *t* tests and a global permutation test (×10,000) of microarray data yielded two main gene clusters up-regulated in EpCAM$^+$ cell lines (HuH1, HuH7, and Hep3B) (cluster I, 524 genes) or in CD90$^+$ cell lines (HLE, HLF, and SK-Hep-1) (cluster II, 366 genes) (Fig. 3C). PLC/PRL/5 showed intermediate gene-expression patterns between EpCAM$^+$ and CD90$^+$ cell lines using this gene set. Pathway analysis indicated that the genes

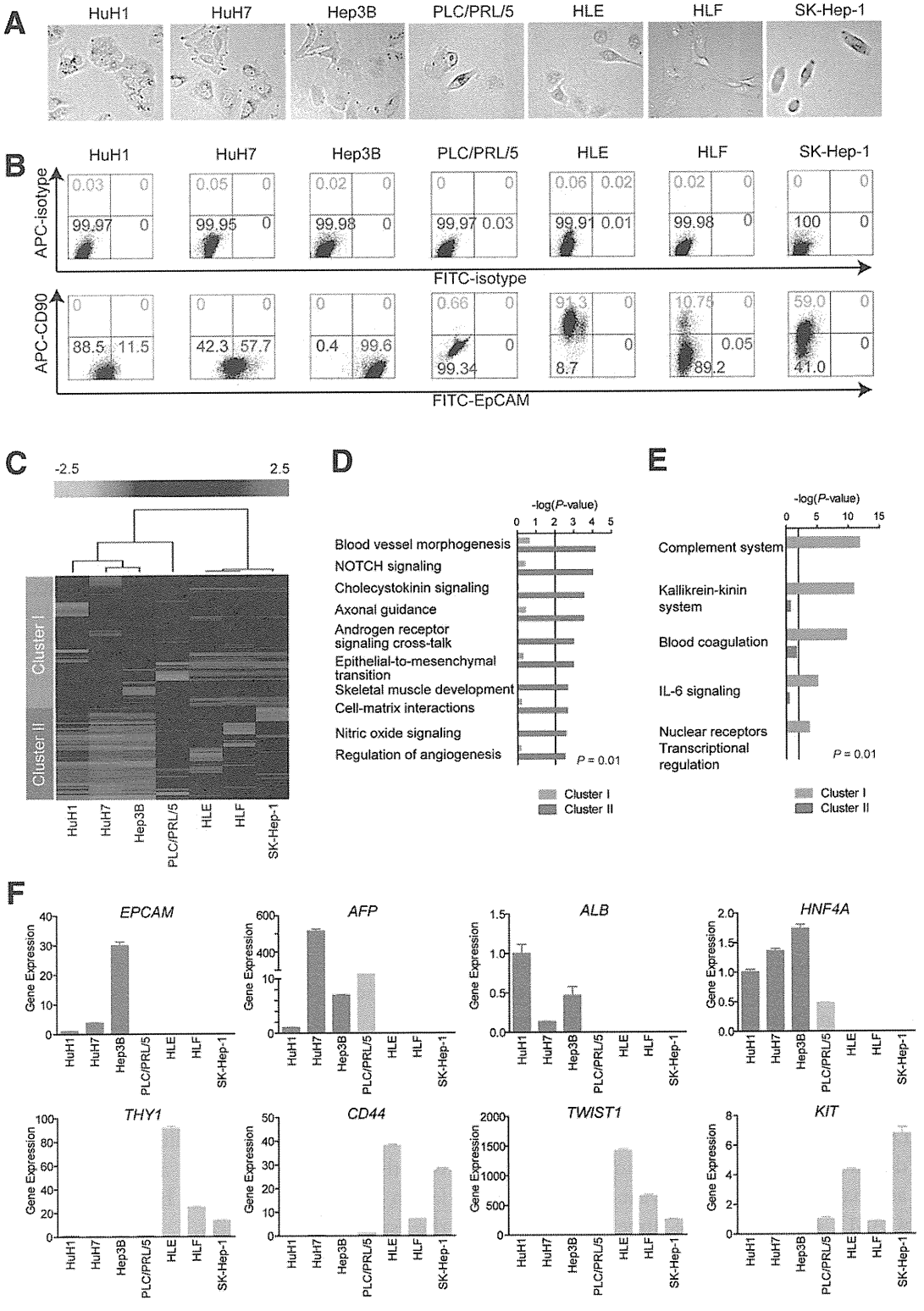

Fig. 3. Characteristics of HCC cell lines defined by EpCAM and CD90. (A) Representative photomicrographs of $EpCAM^{+}CD90^{-}$ and $EpCAM^{-}$ $CD90^{+}$ HCC cell lines. (B) Representative FACS data of $EpCAM^{+}CD90^{-}$ and $EpCAM^{-}$ $CD90^{+}$ HCC cell lines stained with fluorescein isothiocyanate (FITC)-EpCAM and APC-CD90 Abs. (C) Heat-map images of seven HCC cell lines based on 890 EpCAM/CD90-coregulated genes. Each cell in the matrix represents the expression level of a gene in an individual sample. Red and green cells depict high and low expression levels, respectively, as indicated by the scale bar. (D and E) Pathway analysis of EpCAM/CD90-coregulated genes. Canonical signaling pathways activated in cluster I (orange bar) or II (blue bar) with statistical significance ($P < 0.01$) are shown. (F) qPCR of representative differentially expressed genes identified by microarray analysis (C) in seven HCC cell lines.

enriched in cluster II were mainly associated with blood-vessel morpho- and angiogenesis (Fig. 3D). By contrast, the enriched genes in cluster I were significantly associated with known hepatocyte functions ($P < 0.01$) (Fig. 3E). In addition, we identified that the enriched genes in cluster II were significantly associated with neurogenesis, skeletal muscle development, and EMT.

We used qPCR to validate that known hepatic stem cell (HSC) and hepatocyte markers, such as *AFP*, *EPCAM*, *ALB*, and *HNF4A* genes, were up-regulated in $EpCAM^+$ cell lines, but not detected in $CD90^+$ cell lines (Fig. 3F). By contrast, genes associated with mesenchymal lineages and EMT, such as *KIT*, *TWIST1*, *CD44*, and *THY1*, were strongly up-regulated in $CD90^+$ cell lines.

Unique Tumorigenicity and Metastasis Capacity of Distinct CSCs Defined by EpCAM and CD90. We investigated the tumorigenic capacity of $EpCAM^+$ or $CD90^+$ cells by subcutaneously (SC) injecting 1×10^5 sorted cells of four HCC cell lines (HuH1, HuH7, HLE, and HLF) into nonobese diabetic, severe combined immunodeficient (NOD/SCID) mice. We excluded Hep3B cells for the evaluation of tumorigenicity because almost 100% of cells were EpCAM positive. We further excluded SK-Hep-1 cells from the analysis because they potentially originated from endothelial cells.[12] The highly tumorigenic capacities of $EpCAM^+$ and $CD90^+$ cells were reproduced in HuH1, HuH7, and HLF cell lines, compared with marker-negative cells (Fig. 4A). However, HLE cells did not produce SC tumors, even 12 months after transplantation, in NOD/SCID mice. $EpCAM^+$ cells from HuH1 and HuH7 formed larger tumors more rapidly than $CD90^+$ cells from HLF (Fig. 4B). IHC analyses indicated that $EpCAM^+$ cells did not produce $CD90^+$ cells and *vice versa* in these cell lines *in vivo* (Fig. 4C). $CD90^+$ cells showed a high metastatic capacity, whereas $EpCAM^+$ cells showed no metastasis to the lung when SC tumor volume reached approximately 2,000 (HuH1 and HuH7) or 700 mm^3 (HLF) (Fig. 4D). The high metastatic capacity of PLC/PRL/5 cells, which contain a small population of $CD90^+$ cells, was also confirmed after SC injection into NOD/SCID mice (data not shown). $CD90^+$ cells could divide to generate both $CD90^+$ and $CD90^-$ cells, and $CD90^+$ cells showed a high capacity to invade and form spheroids with overexpression of *TWIST1* and *TWIST2*, which are known to activate EMT programs in HLF cells (Supporting Fig. 2A-D).

We next evaluated the tumorigenic/metastatic capacity of $CD45^-$ tumor cells using 12 fresh primary HCC specimens (P1-P12) that had been surgically resected (Table 2). We further evaluated the tumorigenicity of EpCAM/CD90 sorted cells obtained from xenografts derived from primary HCCs (Supporting Fig. 3A). Of these, we confirmed the tumorigenicity of cancer cells obtained from six primary HCCs after SC injection into NOD/SCID mice within 3 months after transplantation (Fig. 5A; Table 2; Supporting Fig. 3B). $EpCAM^+$ cells derived from four HCCs (P4, P7, P13, and P14) showed highly tumorigenic capacities, compared with $EpCAM^-$ cells. $CD90^+$ cells derived from two HCCs showed equal (P12) or more-tumorigenic capacities (P15), compared with $CD90^-$ cells. Tumorigenicity of $EpCAM^+$ cells was observed in three hepatitis C virus (HCV)-related HCCs and an hepatitis B virus (HBV)-related HCC, whereas tumorigenicity of $CD90^+$ cells was observed in two HBV-related HCCs (Tables 1 and 2).

Using unsorted cells, we compared the frequency of $EpCAM^+$ and $CD90^+$ cells in primary and xenograft tumors and found that $EpCAM^+$ cells remained, but $CD90^+$ cells disappeared, in secondary tumors derived from P4 or P7, whereas $EpCAM^+$ cells disappeared, but $CD90^+$ cells remained, in secondary tumors derived from P12 (Fig. 5B). Morphologically, tumorigenic $EpCAM^+$ cells showed an epithelial cell shape, whereas $CD90^+$ cells showed a mesenchymal VEC shape (Fig. 5C and Supporting Fig. 3C). FACS analysis indicated that P12 HCC cells showed abundant expression of vascular endothelial growth factor receptor (VEGFR) 1 and a vascular endothelial marker endoglin (CD105) (Fig. 5D). By contrast, P4 and P7 HCC cells did not express these vascular endothelial markers (data not shown). Lung metastasis was detected in NOD/SCID mice transplanted with P12 HCC cells, but not in mice transplanted with P4 and P7 HCC cells (Fig. 5E,F).

Taken together, these results suggest that the tumorigenic and metastatic capability of primary HCC may depend on the presence of distinct $EpCAM^+$ or $CD90^+$ CSCs. $EpCAM^+$ cells were associated with a high tumorigenic capacity with hepatic epithelial stem cell features, whereas $CD90^+$ cells were related to the metastatic propensity with VEC features.

Suppression of Lung Metastasis Mediated by $CD90^+$ CSCs by Imatinib Mesylate. We previously demonstrated that Wnt/β-catenin signaling inhibitors could successfully attenuate the tumorigenic capacity of $EpCAM^+$ CSCs in HCC.[8,10] To explore the potential molecular targets activated in $CD90^+$ CSCs, we investigated the expression of the known VEC markers, CD105, VEGFR1 (encoded by *FLT1*), and

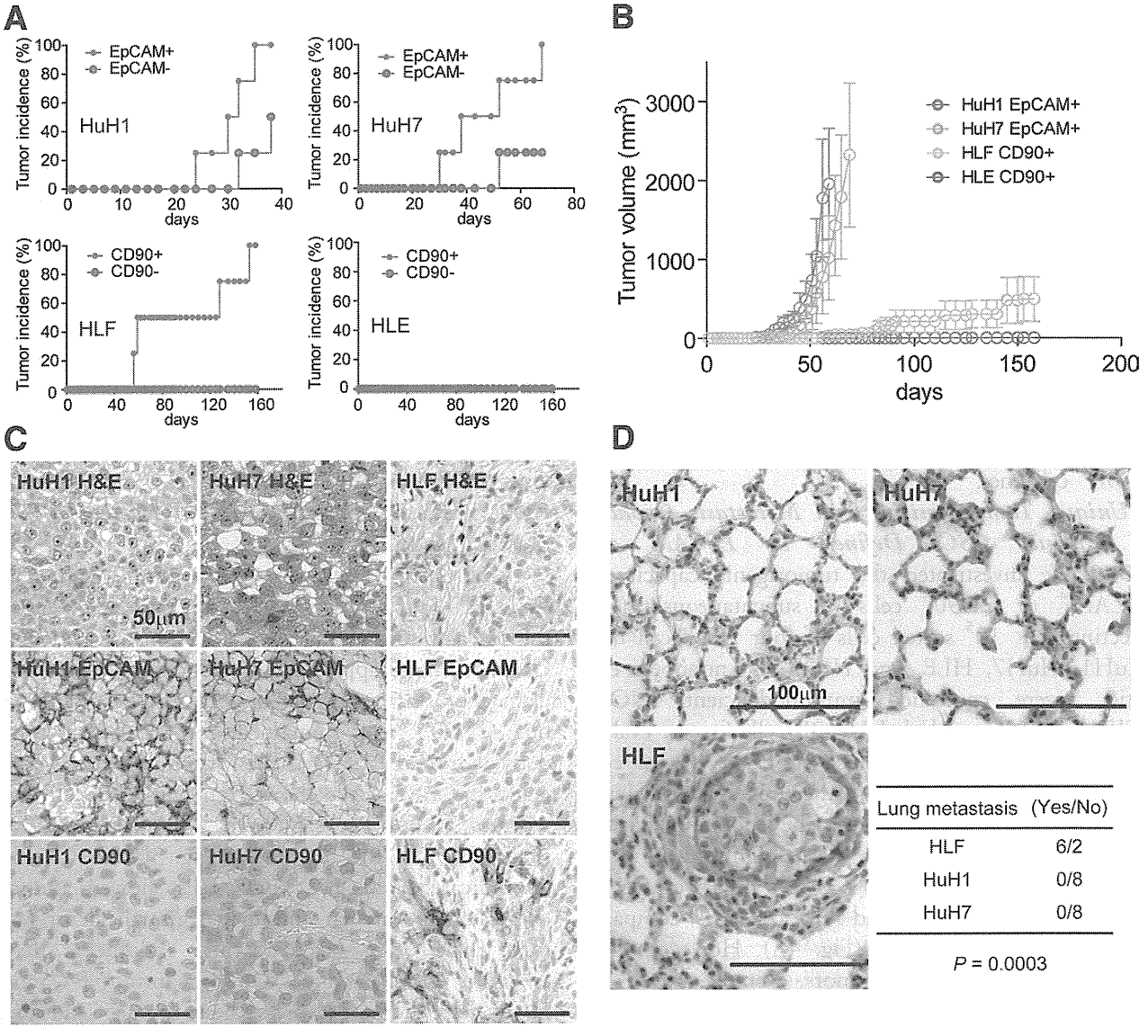

Fig. 4. Distinct tumorigenic/metastatic capacities of HCC cell lines defined by EpCAM and CD90. (A) Tumorigenicity of 1×10^5 cells sorted by anti-EpCAM (HuH1 and HuH7) or anti-CD90 (HLE and HLF) Abs. Data are generated from 8 mice/cell line. (B) Tumorigenic ability of $EpCAM^+$ and $CD90^+$ sorted cells in NOD/SCID mice. Aggressive tumor growth in the SC lesion was observed in $EpCAM^+$ HuH1 or HuH7 cells, compared with $CD90^+$ HLE or HLF cells. $EpCAM^+$ (1×10^5) or $CD90^+$ cells were injected. Tumor-volume curves are depicted as mean ± standard deviation of 4 mice/group. (C) Histological analysis of $EpCAM^+$ or $CD90^+$ cell-derived xenografts. Hematoxylin and eosin (H&E) staining of a SC tumor (upper panels) and IHC of the tumor with anti-EpCAM (middle panels) or anti-CD90 Abs (bottom panels) are shown (scale bar, 50 μm). (D) Metastasis was evaluated macroscopically and microscopically in the left and right lobes of the lung separately in each mouse (n = 4) (scale bar, 100 μm).

c-Kit (encoded by *KIT*), in cell lines and showed that they were abundantly expressed in $CD90^+$ cell lines, but not $EpCAM^+$ cell lines (Fig. 6A). No expression of VEGFR2 was detected in this set of cell lines, suggesting that molecular reagents specifically targeting VEGFR2 may have no effects on $CD90^+$ CSCs. CD44, a stem cell marker that functionally regulates redox status and is a potential target of $CD90^+$ CSCs, was also abundantly expressed in $CD90^+$ cell lines (Supporting Fig. 4A), consistent with previous data.[5,13] No significant difference was detected in the expression of the hematopoietic marker, CD34, or ABCG2 between $EpCAM^+$ and $CD90^+$ cell lines (Supporting Fig. 4A).

Among these molecular targets, we focused on the characterization of c-Kit because the c-Kit tyrosine kinase inhibitor, imatinib mesylate, is readily available, is widely used for the treatment of gastrointestinal stromal tumor with activation of c-Kit, and may have potential antitumor activity against a subset of HCC.[14] We explored the effect of imatinib mesylate on HCC cell lines and found that treatment with 10

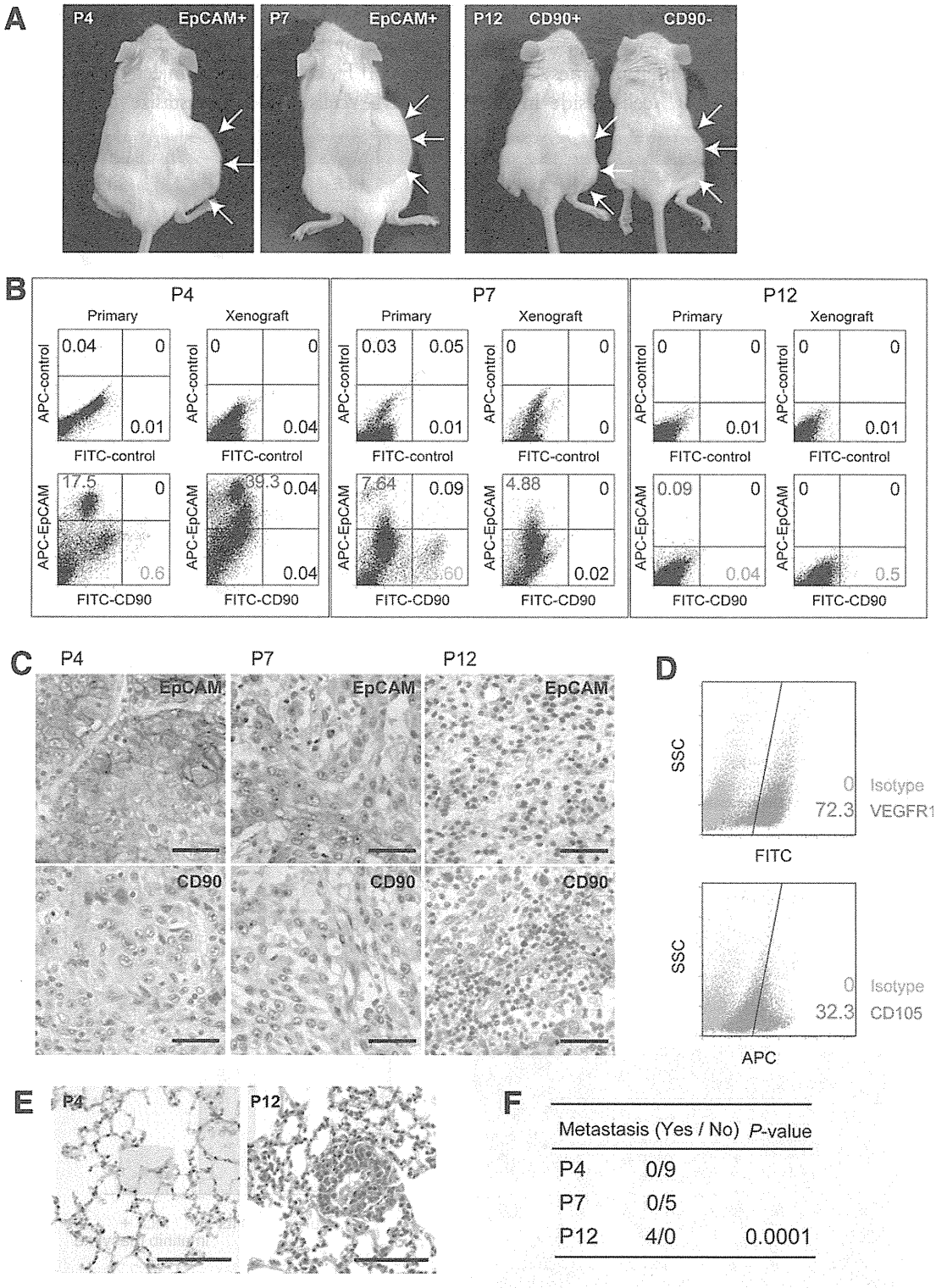

Fig. 5. Tumorigenic/metastatic capacities of EpCAM$^+$ and CD90$^+$ cells in primary HCC. (A) Representative NOD/SCID mice with SC tumors (white arrows) from EpCAM$^+$ P4 or P7 cells (left and middle panels) and CD90$^+$ or CD90$^-$ P12 cells (right panel). (B) FACS analysis of CD90 and EpCAM staining in primary HCCs and the corresponding secondary tumors developed in NOD/SCID mice. Unsorted cells (1×10^6 cells in P4 and P7 or 1×10^5 cells in P12) were SC injected to evaluate the frequency of each marker-positive cell in primary and secondary tumors. (C) IHC analysis of EpCAM and CD90 in primary HCCs P4, P7, and P12 (scale bar, 50 μm). (D) FACS analysis of VEGFR1 (Alexa488) and CD105 (APC) in primary HCC P12. (E) Hematoxylin and eosin staining of lung tissues in P4 and P12 (scale bar, 200 μm). (F) Frequency of lung metastasis in NOD/SCID mice SC transplanted using unsorted primary HCC cells.

μM reduced cell proliferation and spheroid formation in CD90$^+$ cell lines, but had no effect on EpCAM$^+$ cell lines (Supporting Fig. S4B,C).

We further explored the effect of imatinib mesylate *in vivo*. Because EpCAM$^+$ and CD90$^+$ cells reside in the primary HCC, but not in established cell lines, we SC injected HuH7 and HLF cell lines to generate tumors organized by EpCAM$^+$ and CD90$^+$ CSCs. Interestingly, when HLF cells were coinjected with HuH7 cells, EpCAM$^+$ cells could metastasize to the lung, whereas